

Diagnostic performance of cone-beam computed tomography on detection of mechanically-created artificial secondary caries

Arnon Charuakkra, Sangsom Prapayasatok, Apirum Janhom, Surawut Pongsiriwet, Karune Verochana, Phattaranant Mahasantipiya

Division of Oral and Maxillofacial Radiology, Department of Oral Biology and Diagnostic Sciences, Faculty of Dentistry, Chiang Mai University, Chiang Mai, Thailand

ABSTRACT

Purpose : The aim of this study was to compare the diagnostic accuracy of cone-beam computed tomography (CBCT) images and bitewing images in detection of secondary caries.

Materials and Methods : One hundred and twenty proximal slots of Class II cavities were randomly prepared on human premolar and molar teeth, and restored with amalgam (n=60) and composite resin (n=60). Then, artificial secondary caries lesions were randomly created using round steel No. 4 bur. The teeth were radiographed with a conventional bitewing technique and two CBCT systems; Pax-500ECT and Promax 3D. All images were evaluated by five observers. The area under the receiver operating characteristic (ROC) curve (A_z) was used to evaluate the diagnostic accuracy. Significant difference was tested using the Friedman test (p value < 0.05).

Results : The mean A_z values for bitewing, Pax-500ECT, and Promax 3D imaging systems were 0.882, 0.995, and 0.978, respectively. Significant differences were found between the two CBCT systems and film ($p=0.007$). For CBCT systems, the axial plane showed the greatest A_z value.

Conclusion : Based on the design of this study, CBCT images were better than bitewing radiographs in detection of secondary caries. (*Imaging Sci Dent 2011; 41 : 143-50*)

KEY WORDS : Dental Caries; Cone Beam CT; Radiography, Bitewing; Diagnosis

Introduction

Cone-beam computed tomography (CBCT) has been developed as a new imaging modality for dentists to diagnose various diseases and to determine treatment plan options. It can display the images in axial, sagittal, and coronal planes, as well as permitting three-dimensional (3D) image reconstruction. Therefore, CBCT is widely used in several dental applications.¹ Recently, there have been studies on the accuracy in detection of caries using CBCT.²⁻⁹ However, the effectiveness of CBCT in caries

detection has been still equivocal.

Akdeniz et al² found that limited cone beam computed tomography (LCBCT) was better to assess the depth of proximal caries than intra-oral digital imaging systems using storage phosphor plate sensors and film. The 3DX Accutomo system (Mortita, Kyoto, Japan), one of the CBCT systems, was reported to show significantly higher sensitivity than 2D images in detecting proximal dentin caries.^{4,5} For proximal enamel caries, Young et al⁵ found that the 3DX Accutomo was a superior imaging modality to intra-oral digital imaging systems using charge coupled device (CCD) sensors. Kayipmaz et al⁷ stated that CBCT images could detect occlusal caries better than conventional films and storage phosphor plates, whereas no significant difference was found for proximal caries. Kamburoglu et al⁹ found that CBCT images improved the detection of occlusal caries in deep enamel, superficial dentin, and

*This study was funded by the Faculty of Dentistry, Chiang Mai University, Thailand. Received June 23, 2011; Revised July 4, 2011; Accepted July 6, 2011

Correspondence to : Dr. Arnon Charuakkra
Division of Oral and Maxillofacial Radiology, Department of Oral Biology and Diagnostic Sciences, Faculty of Dentistry, Chiang Mai University Suthep Road, T. Suthep, Muang District, Chiang Mai, 50200, Thailand
Tel) 66-53-944453, Fax) 66-53-222844, E-mail) arnon_cha903@hotmail.com

deep dentin compared with CCD images. On the contrary, Tsuchida et al³ stated that an LCBCT system, the 3D Accuitomo, did not significantly enhance accuracy in detecting proximal carious lesions compared with film radiography (Insight F-speed film, Eastman Kodak Company, Rochester, NY, USA). Haiter-Neto et al⁴ demonstrated that NewTom 3G system (Quantitative Radiology, Verona, Italy) (9 inch and 6 inch FOV) had significantly lower specificities than film and Digora-fmx (Soredex, Tuusula, Finland) for proximal caries detection; besides, 3Dx Accuitomo images were not significantly different from film and Digora-fmx images in detecting proximal caries. Zhang et al⁸ reported that the accuracy of non-cavitated caries detection using the Promax 3D system (Planmeca Oy, Helsinki, Finland) and the Kodak 9000 3D system (Carestream Health, Rochester, NY, USA) was not significantly different from that achieved using phosphor plate and film-based intraoral images (Kodak E speed films, Carestream Health, Rochester, NY, USA). They also suggested that CBCT examination should not, therefore, be recommended exclusively for proximal caries diagnosis.

Secondary caries is a type of caries frequently found in restored teeth and is defined as a type of caries occurring at the margin of an existing restoration, running along the cavity walls, especially in areas of plaque stagnation. It is rare on the occlusal surface because the occlusal margin of a restoration is cleansable. For this reason, the cervical margins of restorations are commonly affected.¹⁰ Mjör and Toffenetti¹¹ stated that 50%-60% of restorations had been replaced because of the secondary caries. Bitewing radiograph plays an important role in detecting secondary caries. However, the superimposition of structures on the caries in the line of the central ray may cause misinterpretation. In addition, the radiopacity of a restoration serves to affect the accuracy of the radiographic detection of secondary caries.¹²

To our knowledge, no study has been carried out comparing the diagnostic accuracy between CBCT and intraoral images for secondary caries detection. The only study related to Tuned Aperture Computed Tomography (TACT) was by Nair et al¹³ who found that TACT provided more effectiveness than either Ektaspeed Plus film (Eastman Kodak Company, Rochester, NY, USA) and a direct digital system (Trophy RVGTM, Trophy Radiology, Marietta, GA, USA) for detection of secondary caries. Therefore, the objective of this study was to compare the diagnostic accuracy of two CBCT systems and bitewing radiographs in the detection of secondary caries.

Materials and Methods

One hundred and four extracted sound human premolar and molar teeth were used in this study. Proximal slots of Class II cavities were randomly prepared on the mesial and/or distal surfaces of the teeth. The gingival floor of the cavity was placed 2 mm coronal to the CEJ. The slot preparations were divided into two groups, according to the type of restoration. The first group was restored by amalgam and the other group by composite resin (FiltekTM Z350, 3M ESPE Dental Products, St. Paul, MN, USA), resulting in 60 amalgam and 60 composite resin restorations. For composite resin restoration, the cavities were etched for 15 seconds, and the bonding agent was applied with curing time of 40 seconds. In each group, artificial secondary caries lesions were created in half of the restorations. The artificial caries lesions were created using round steel No. 4 burs (1.4 mm diameter), at the midpoint, beneath the gingival margin of the restorations (Fig. 1). The drilled cavities were then filled with pink wax. The teeth were subsequently arranged in an anatomical arch form in plastic blocks and mounted in plaster; the proximal contacts consisted of two premolars and two molars in each block.

All of the blocks were radiographed by two CBCT systems, Pax-500ECT (Vatech, Yongin, Korea) and ProMax 3D (Planmeca Oy, Helsinki, Finland) and a film-based bitewing technique. The soft tissue equivalent was placed adjacent to the dental blocks and was located between the source and the dental blocks. The Pax-500ECT CBCT machine was operated at 85 kVp and 3.5 mA with 5 × 5 cm FOV. The acquired data were reconstructed with 1 mm slice thickness. Ez3D Viewer (Vatech, Yongin, Korea) software was used to evaluate the resulting images in three orthogonal planes. The images were displayed using a

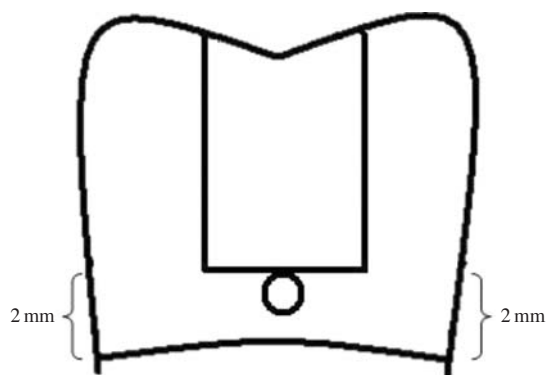


Fig. 1. The illustration shows artificial caries prepared at the gingival floor and sealed with pink wax.

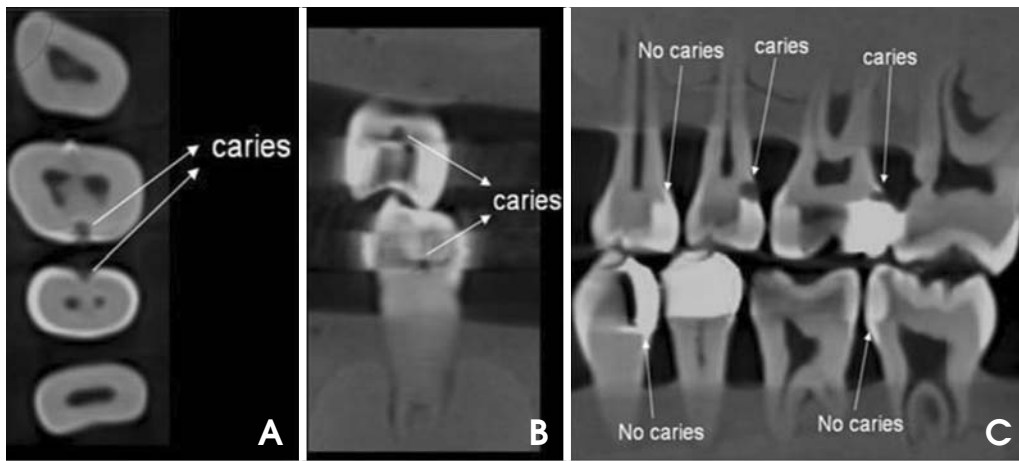


Fig. 2. Examples of CBCT images demonstrates either secondary caries present or absent. A. Axial plane. B. Coronal plane. C. Sagittal plane.

laptop computer (Pavilion dv9500, Hewlett Packard, Palo Alto, CA, USA) with a 14-inch monitor with a resolution of 1440×900 pixels. The ProMax 3D CBCT machine was operated at 84 kVp and 4 mA with an 8×8 cm FOV. The acquired data were reconstructed with 0.48 mm slice thickness. Romexis Viewer (Planmeca Oy, Helsinki, Finland) software was used to evaluate the resulting images in three orthogonal planes. The images were displayed and the same laptop computer previously mentioned was used. Examples of CBCT images are displayed in Figure 2.

For the bitewing radiograph, each dental model was radiographed using F-speed films (Insight Dental Film, Eastman Kodak Company, Rochester, NY, USA), with an intraoral x-ray machine, Planmeca Intra (Planmeca Oy, Helsinki, Finland) at 66 kVp, 8 mA and 0.2 sec. The soft tissue equivalent was also used. The films and dental models were set on a wooden bench to ensure reproducible beam geometry. The source-film distance and object-film distance were 355 mm and 20 mm, respectively. The exposed films were then processed using an automatic film processor, the Clarimat 300[®] (Gendex, London, UK). The processed films were mounted in film mounting frames for interpretation. Examples of bitewing images are displayed in Figure 3.

Five experienced dentists served as the observers; all of them had at least ten years experience in the oral diagnostic field. Four were oral radiologists, and the other one had Thai Board Certification in Oral Diagnostic Science. The observers were provided with a training session to familiarize them with the CBCT software viewers. Verbal instructions and demonstrations of the basic CBCT software for the Ez3D Viewer and Romexis Viewer were given to each observer before image evaluation. Examples of the images with the presence or absence of artificial secondary caries

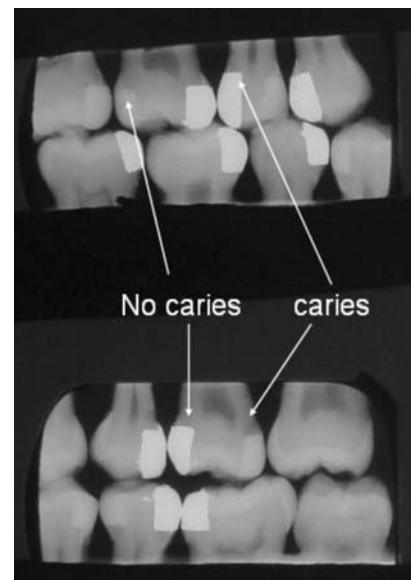


Fig. 3. Examples of bitewing images demonstrate either secondary caries present or absent

on both CBCT and bitewing images were shown to each observer. Image viewing was conducted in a dimly lit room with no time restrictions on evaluation. For bitewing interpretation, the observers were asked to score twice, with a 1-week interval between viewings to eliminate memory bias and fatigue. For the CBCT interpretation, since the observers needed to scroll the images in several planes and the procedure took a long time, only 10% of the samples were evaluated a second time to analyze intra-observer agreement with a 1-week interval between viewings.

The sequence of the image interpretation was the same for all observers, starting with the bitewing, followed by the CBCT from the Pax-500ECT, and then the CBCT from

the Promax 3D. After the calibration session, all observers were asked to score the images, in terms of whether or not the artificial secondary caries was present, using a 5-point confidence scale (1=caries definitely not present, 2=caries probably not present, 3=unsure if caries is absent or present, 4=caries probably present and 5=caries definitely present). The observers were asked to score the images in each plane separately, and gave a final score for each slot restoration.

The area under the receiver operating characteristic (ROC) curve (A_z) was used to evaluate diagnostic accuracy. Differentiation of A_z areas between the bitewings and the two CBCT systems was conducted using the Friedman test. Pair-wise comparisons were made when significant differences were found with the Friedman test. The A_z values regarding the CBCT imaging planes (axial, coronal and sagittal planes) and the types of restoration (amalgam and composite resin) were analyzed using the Friedman test and Wilcoxon signed-ranks test. Kappa analysis was used to test for inter- and intra-examiner agreement. Differences were considered to be statistically significant when $p < 0.05$.

Results

The ROC curves are demonstrated in Figure 4. The mean A_z values for bitewings, Pax-500ECT, and Promax 3D imaging systems were 0.882, 0.995, and 0.978, respectively

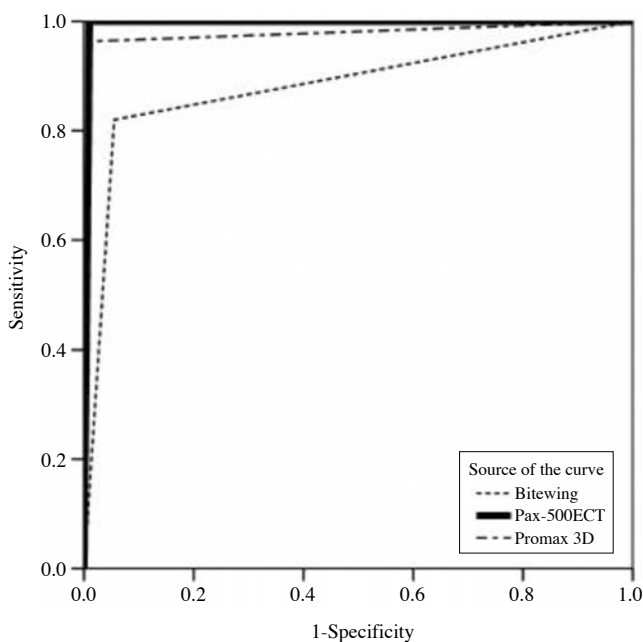


Fig. 4. ROC curves represent pooled radiographic scores for five observers diagnosing secondary caries in connection with imaging modalities.

(Table 1). Significant differences were found among Pax-500ECT, Promax 3D and bitewing films (Friedman test, $p=0.007$). The results of the pair-wise comparisons between the bitewings and the two CBCT systems, and between the Pax-500ECT and the Promax 3D systems were significantly different ($p < 0.05$).

The mean A_z values for Pax-500ECT and Promax 3D in axial, coronal, and sagittal planes are demonstrated in Table 2. There was a significant difference among the planes with the Pax-500ECT system ($p=0.037$), whereas no significant difference was found among the planes with the Promax 3D system ($p=0.529$). Of all three planes, the axial plane showed the largest A_z value for both CBCT systems.

When the types of restoration were evaluated separately, the A_z values were similar to those of the overall results for all three imaging modalities (Table 3). However, when comparing amalgam and composite resin restorations for each modality, no significant difference was found with the bitewings ($p=0.686$), the Pax-500ECT ($p=0.317$) or Promax 3D ($p=0.141$) systems.

The kappa value for intra-observer agreement ranged between 0.659 and 0.848 for bitewings, and it was equal to 1.000 for both CBCT systems. For inter-observer agreement, the kappa value ranged between 0.400 and 0.780 for bitewings, and it was equal to 1.000 for both CBCT systems.

Table 1. Areas under the ROC curves of bitewing and CBCT systems

Observer	Bitewing	Pax-500ECT	Promax 3D
1	0.921	1.000	0.992
2	0.862	0.975	0.967
3	0.825	1.000	0.975
4	0.896	1.000	0.975
5	0.908	1.000	0.983
Mean	0.882	0.995	0.978

Table 2. Areas under the ROC curves of Pax-500ECT and Promax 3D in axial, coronal and sagittal planes

	Axial plane	Coronal plane	Sagittal plane
Pax-500ECT	0.996	0.965	0.973
Promax 3D	0.975	0.966	0.945

Table 3. Areas under the ROC curves for amalgam and composite resin restorations

	Bitewing	Pax-500ECT	Promax 3D
Amalgam	0.885	0.996	0.983
Composite resin	0.879	0.993	0.973

Discussion

The present study revealed that the diagnostic accuracy of the two CBCT systems (A_z values=0.995 and 0.978) was significantly higher than that of bitewing radiography (A_z value=0.882) in the detection of artificial secondary caries. The explanation for this result is that CBCT systems display multi-planar images such as axial, coronal, and sagittal planes, and using these multiple planes, the lesions could be found without superimposition on other nearby structures or even on the restoration itself. On the other hand, on the bitewing radiographs, the artificial secondary caries might be hidden by the restorations due to superimposition of radiopaque structures or restorations on the caries along the line of the central ray. Furthermore, an additional drawback of bitewing radiographs for the detection of secondary caries in clinical situations is the difficulty of film placement, which varies from person to person due to the differences in anatomical structures. Incorrect film position and unsuitable beam angulation can cause proximal angular overlapping, resulting in radiographic misinterpretation. To date, no study on the detection of secondary caries using CBCT has been reported. Nevertheless, a study by Young et al⁵ reported that CBCT images from the 3DX Accuitomo system (Mortita, Kyoto, Japan) showed higher sensitivity than 2D images in detecting dentin proximal caries. In our study, the artificial secondary caries that we created was in dentin and at the proximal surface.

The A_z value for bitewing imaging (0.882) in our study was similar to that of the study by Espelid et al.¹⁴ However, the secondary caries in their study was natural, whereas our lesions were mechanically created. The A_z value for bitewing imaging showed a lower value compared with CBCT systems. There are some possible explanations for this result. First, the teeth arranged in an anatomical arch form in plastic blocks were tilted either buccally or lingually for the establishment of stability of occlusion. This might have led to the artificial secondary caries being hidden by the restorations due to superimposition of radiopaque structures or restorations on the caries along the line of the central ray. Second, the Mach band effect might have resulted in misinterpretation of caries. The Mach band effect is an optical illusion occurring when there is a sharply defined density difference,¹ such as the junction between the restorations and underlying tooth structure. It might have appeared as a dark band at such junctions in this study. This Mach band effect might have contributed to the number of false positive interpretations. A study by Espelid and

Tveit¹⁵ reported a high percentage (12%) of misdiagnosis of secondary caries under intact restorations, possibly due to Mach band illusions.

In comparing CBCT planes, the axial plane showed the largest A_z values in our study. Our hypothesis was that when the observers observed the images, if they scrolled through the images in a sequence from the normal root structure, through the margin to the body of the restoration, the observers then could easily assess the starting point of the artificial secondary caries that was not obscured by the adjacent restorations. On the coronal and sagittal planes, the images of the lesions and restorations were always found simultaneously, and the artifacts from the restorations might have disturbed the radiographic interpretation.

Regarding the types of restorations, the A_z values for the amalgam and composite resin restorations were not significantly different for each imaging modality. The results of the bitewing radiographs in our study did not agree with those of previous studies using conventional radiographs to detect secondary caries. A few studies^{13,14,16} demonstrated that secondary caries occurring under composite resin restorations was more accurately diagnosed than under amalgam, particularly when the radiopacity of the composite resin was equal to or greater than that of enamel. In our study, we found that the density of composite resin was similar to that of enamel. For the CBCT systems, we first postulated that the artifacts from the amalgam restoration would impair the radiographic interpretation. Surprisingly, the A_z values of amalgam and composite resin restorations were not significantly different for either CBCT system. Many factors in the design of our study might have affected these results.

The artificial secondary caries in our study was created using round steel No. 4 burs (1.4 mm diameter) and located at the mid-gingival floor. As a result, large, round-shaped, clearly defined caries at this specific location might have resulted in interpretations that might have been different from “true” interpretations in a clinical situation. Kang et al¹⁷ compared the ability to detect mechanically-created defects and natural dental carious cavitations on the proximal surfaces of extracted teeth. They found that the mechanically-created caries was radiographically detected 2.92 times more reliably than natural caries cavitations because the radiographic features of mechanically-created caries provided higher contrast than that of natural caries. The calibration session might have been another complicating factor. In this study, before the observers were asked to score the images, examples of images with caries, either present or absent, were shown to them in every plane of

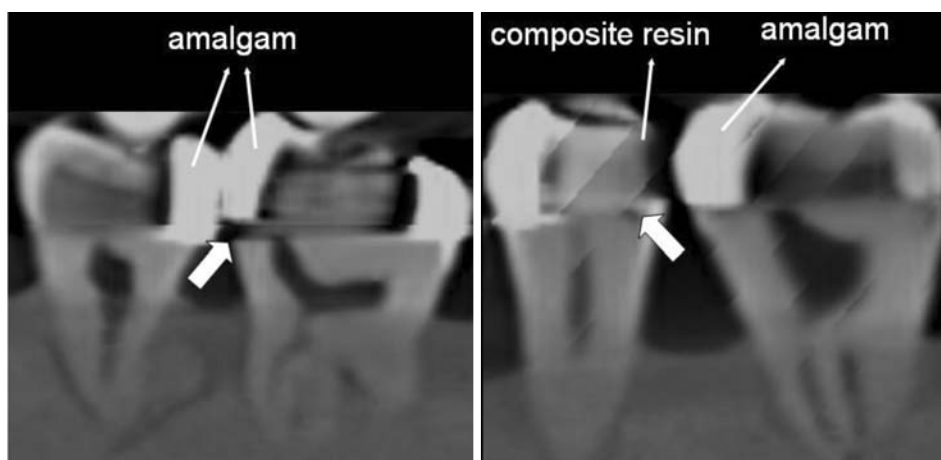


Fig. 5. Examples of CBCT images in sagittal plane in which misinterpretation of secondary caries occurred. Thick arrows point at the surfaces that gave false positive results.

both CBCT systems. The observers were informed that only the caries which specifically had the round shape and which were located at the mid-gingival floor would be interpreted as representing caries present. Radiolucencies with other shapes that might be found in other locations would not be included as caries in this study. Therefore, these experimental design factors (the specific shape, size and location of the mechanically-created caries, and the fact that the observers were asked to evaluate only some specified proximal surfaces with specific shape and location correlated to the CBCT image samples) might have biased the observers, and might have resulted in very high A_z values (nearly 1.000) for both CBCT systems, and might have eliminated the confounding factor of artifacts from amalgam restorations. Matteson et al¹⁶ studied on the effect of lesion size in detection of recurrent caries and found that large caries lesions were detected more accurately than small ones. Another study by Nair et al¹⁸ reported that secondary caries located at the mid-gingival floor was more easily detected than at other locations. Since the purpose of this study was first to examine the effectiveness of CBCT on the detection of secondary caries, we eliminated as many other confounding factors as possible. Hence, large caries lesions at the mid-gingival floor were designed. In the clinical situation, caries can occur anywhere with various shapes, sizes and locations; therefore, future research on secondary caries by CBCT should include these confounding factors that may affect the interpretation. Instead of using burs to create well-defined artificial caries lesions, there are other methods to create artificial caries that simulate the clinical situation, for instance, bacterial challenge or acidified broth.¹⁹ In case of creating artificial dental caries using dental bur, we recommend smaller burs than No. 4.



Fig. 6. The CBCT image in the sagittal plane shows the artifacts (arrow) from the adjacent amalgam restoration that could be misinterpreted as secondary or remnant caries.

Several studies showed that radiopaque materials, such as gutta percha,²⁰ orthodontic brackets,²¹ surgical plates and pins,²² dental implants,²³ and metal crowns²⁴ produce artifacts in CBCT images that may affect radiographic interpretation. In our study, amalgam, which causes artifacts in CBCT images, did not affect the detection of secondary caries as much as it did in bitewing images. This result might be due to the large artificial caries used in this study, therefore the amount of artifacts from the amalgam restoration might not have been large enough to disturb the visibility of secondary caries on CBCT images. However, only eight restorations from both CBCT systems were radiographically misinterpreted in our study (Fig. 5). Among them, we found that seven of them had amalgam



Fig. 7. The Promax 3D system CBCT image (A) demonstrates a greater amount of artifacts than that of the Pax-500ECT system (B).

proximity. The other one had natural tooth contact. Therefore, the author supposed that the nearby amalgam restoration might possibly affect the diagnostic accuracy of secondary caries in CBCT images. Future research on this issue should be performed.

Remnant caries can be sometimes considered as secondary caries. In this study, secondary caries was defined as a type of caries occurring at the margin of an existing restoration.¹⁰ From our observation, the artifacts seen as dark streaks beneath the amalgam restoration were usually revealed on the CBCT images; consequently, the artifacts could be misinterpreted as secondary or remnant caries (Fig. 6).

There were a few studies comparing the diagnostic accuracy of different CBCT systems in detection of proximal caries. Qu et al⁶ compared five CBCT systems with different types of detectors and fields of view (FOVs): NewTom 9000 (Quantitative Radiology, Verona, Italy), 3DX Accuitomo, Kodak 9000 3D (Carestream Health, Rochester, NY, USA), ProMax 3D, and DCT PRO (Vatech, Yongin, Korea). They found that neither the detector nor the FOV employed by the CBCT systems had an impact on the detection accuracy of proximal enamel or dentin caries. Zhang et al⁸ also showed that there was no significant difference in detecting non-cavitated proximal enamel and dentin caries between images produced by Kodak 9000 3D and ProMax 3D systems, with different detectors, fields of view, voxel sizes, or slice thicknesses. Another study by Haiter-Neto et al⁴ demonstrated that NewTom 3G system (Quantitative Radiology, Verona, Italy) (12 inch, 9 inch, and 6 inch FOVs) had significantly lower sensitivity than the 3DX Accuitomo system (3 × 4 cm FOV) in detection

of proximal enamel and dentin caries. In our study, the Pax-500ECT system demonstrated higher A_z values than those of the Promax 3D for the diagnostic accuracy of secondary caries. The Pax-500ECT system has a smaller FOV (5 × 5 cm) than that of the Promax 3D (8 × 8 cm). Two pairs of dental blocks were radiographed in the Promax 3D system, whereas only one pair was radiographed in the Pax-500ECT, due to its limited FOV. Accordingly, the artifacts from one side may affect the image of the other side, resulting in lower A_z values. In addition, more artifacts were observed in the Promax 3D system than in the Pax-500ECT system (Fig. 7).

In this study, the inter- and intra-observer agreement kappa values for the CBCT systems were higher than those for bitewing radiographs. Both inter- and intra-observer agreements for the CBCT systems were equal to 1.000. These results might be originated from the thin slice CBCT images of tooth structures, resulting in high contrast between caries lesions and sound tooth structures; less misinterpretation then occurred with high kappa values.²

Finally, we performed this study not aiming to use or to support CBCT images in detection of secondary caries. However, a provisional guideline for CBCT application (produced by the SEDENTEXCT project in Europe in 2009)²⁵ states that “CBCT images must undergo a thorough clinical evaluation (‘radiological report’) of the entire image dataset.” It is, therefore, possible to find suspected secondary caries on CBCT images prescribed for other dental purposes such as implants, root fractures, complex maxillofacial fractures, and so on. Our study might, at least, indicate that CBCT images had some efficiency but still had some limitations in detection of secondary caries.

In conclusion, based on the design of this study, in which the mechanically-created artificial secondary caries lesions were large, round, and located at the mid-gingival floor of the restorations, CBCT images were better than bitewing images in detection of secondary caries. Nevertheless, for the clinical application of CBCT in detection of secondary caries, more research should be performed.

Acknowledgement

The author would like to thank Dr Narumanas Korwanich for consultation of statistical analysis, and Dr Attavit Pisitanusorn for the Pax-500ECT CBCT machine usage. The author would also like to thank Dr. M. Kevin O Carroll, Professor Emeritus of the University of Mississippi School of Dentistry, USA and Faculty Consultant at Chiang Mai University Faculty of Dentistry, Thailand, for his assistance in the preparation of the manuscript in English.

References

1. Scarfe WC, Farman AG. Cone-beam computed tomography. In: White SC, Pharoah MJ. *Oral radiology: principle and interpretation*. 6th ed. St. Louis: Mosby; 2009. p. 225-42.
2. Akdeniz B, Gröndahl H, Magnusson B. Accuracy of proximal caries depth measurements: comparison between limited cone beam computed tomography, storage phosphor and film radiography. *Caries Res* 2006; 40: 202-7.
3. Tsuchida R, Araki K, Okano T. Evaluation of a limited cone-beam volumetric imaging system: comparison with film radiography in detecting incipient proximal caries. *Oral Surg Oral Med Oral Pathol Oral Radiol Endod* 2007; 104: 412-6.
4. Haiter-Neto F, Wenzel A, Gotfredsen E. Diagnostic accuracy of cone beam computed tomography scans compared with intraoral image modalities for detection of caries lesions. *Dentomaxillofac Radiol* 2008; 37: 18-22.
5. Young SM, Lee JT, Hodges RJ, Chang TL, Elashoff DA, White SC. A comparative study of high-resolution cone beam computed tomography and charge-coupled device sensors for detecting caries. *Dentomaxillofac Radiol* 2009; 38: 445-51.
6. Qu X, Li G, Zhang Z, Ma X. Detection accuracy of in vitro approximal caries by cone beam computed tomography images. *Eur J Radiol* 2011; 79: e24-7.
7. Kayipmaz S, Sezgin OS, Saricaoglu ST, Can G. An in vitro comparison of diagnostic abilities of conventional radiography, storage phosphor, and cone beam computed tomography to determine occlusal and approximal caries. *Eur J Radiol* 2011; 80: 478-82.
8. Zhang ZL, Qu XM, Li G, Zhang ZY, Ma XC. The detection accuracies for proximal caries by cone-beam computerized tomography, film, and phosphor plates. *Oral Surg Oral Med Oral Pathol Oral Radiol Endod* 2011; 111: 103-8.
9. Kamburoglu K, Murat S, Yüksel SP, Cebeci AR, Paksoy CS. Occlusal caries detection by using a cone-beam CT with different voxel resolutions and a digital intraoral sensor. *Oral Surg Oral Med Oral Pathol Oral Radiol Endod* 2010; 109: e63-9.
10. Kidd EA. Diagnosis of secondary caries. *J Dent Educ* 2001; 65: 997-1000.
11. Mjör IA, Toffenetti F. Secondary caries: a literature review with case reports. *Quintessence Int* 2000; 31: 165-79.
12. Imperiano MT, Khoury HJ, Pontual ML, Montes MA, Silveira MM. Comparative radiopacity of four low-viscosity composites. *Braz J Oral Sci* 2007; 6: 1278-82.
13. Nair MK, Tyndall DA, Ludlow JB, May K. Tuned aperture computed tomography and detection of recurrent caries. *Caries Res* 1998; 32: 23-30.
14. Espelid I, Tveit AB, Erickson RL, Keck SC, Glasspoole EA. Radiopacity of restorations and detection of secondary caries. *Dent Mater* 1991; 7: 114-7.
15. Espelid I, Tveit AB. Diagnosis of secondary caries and crevices adjacent to amalgam. *Int Dent J* 1991; 41: 359-64.
16. Matteson SR, Phillips C, Kantor ML, Leinedecker T. The effect of lesion size, restorative material, and film speed on the detection of recurrent caries. *Oral Surg Oral Med Oral Pathol* 1989; 68: 232-7.
17. Kang B-C, Farman AG, Scarfe WC, Goldsmith LJ. Mechanical defects in dental enamel vs. natural dental caries: observer differentiation using Ektaspeed Plus film. *Caries Res* 1996; 30: 156-62.
18. Nair M, Tyndall D, Ludlow J, May K, Ye F. The effects of restorative material and location on the detection of simulated recurrent caries. A comparison of dental film, direct digital radiography and tuned aperture computed tomography. *Dentomaxillofac Radiol* 1998; 27: 80-4.
19. Grossman ES, Matejka JM. Histological features of artificial secondary caries adjacent to amalgam restorations. *J Oral Rehabil* 1999; 26: 737-44.
20. Hassan B, Metska ME, Ozok AR, van der Stelt P, Wesselink PR. Detection of vertical root fractures in endodontically treated teeth by a cone beam computed tomography scan. *J Endod* 2009; 35: 719-22.
21. Sanders MA, Hoyjberg C, Chu CB, Leggitt VL, Kim JS. Common orthodontic appliances cause artifacts that degrade the diagnostic quality of CBCT Images. *J Calif Dent Assoc* 2007; 35: 850-7.
22. Cevidanes LH, Tucker S, Styner M, Kim H, Chapuis J, Reyes M, et al. Three-dimensional surgical simulation. *Am J Orthod Dentofacial Orthop* 2010; 138: 361-71.
23. Razavi T, Palmer RM, Davies J, Wilson R, Palmer PJ. Accuracy of measuring the cortical bone thickness adjacent to dental implants using cone beam computed tomography. *Clin Oral Implants Res* 2010; 21: 718-25.
24. Zhang Y, Zhang L, Zhu X, Lee A, Chambers M, Dong L. Reducing metal artifacts in cone-beam CT images by preprocessing projection data. *Int J Radiat Oncol Biol Phys* 2007; 67: 924-32.
25. SEDENTEXCT Project [Internet]. Radiation protection: cone beam CT for dental and maxillofacial radiology. Evidence based guidelines 2011 [cited 2011 Oct 24]. Available from: http://www.sedentexct.eu/files/guidelines_final.pdf.